

See discussions, stats, and author profiles for this publication at: <https://www.researchgate.net/publication/257648481>

Fullerene “Superhalogen” Radicals: the Substituent Effect on Electronic Properties of 1,7,11,24,27-C₆₀X₅

ARTICLE in CHEMISTRY - A EUROPEAN JOURNAL · SEPTEMBER 2013

Impact Factor: 5.73 · DOI: 10.1002/chem.201301234 · Source: PubMed

CITATIONS

3

READS

47

7 AUTHORS, INCLUDING:



Tyler T Clikeman

Colorado State University

11 PUBLICATIONS 17 CITATIONS

SEE PROFILE



Stanislav Avdoshenko

Leibniz Institute for Solid State and Materia...

70 PUBLICATIONS 705 CITATIONS

SEE PROFILE



Alexey A Popov

Leibniz Institute for Solid State and Materia...

188 PUBLICATIONS 3,412 CITATIONS

SEE PROFILE



Olga V. Boltalina

Colorado State University

268 PUBLICATIONS 4,242 CITATIONS

SEE PROFILE

Fullerene “Superhalogen” Radicals: the Substituent Effect on Electronic Properties of 1,7,11,24,27- $C_{60}X_5$

Tyler T. Clikeman,^[a] S. H. M. Deng,^[c] Stanislav Avdoshenko,^[d] Xue-Bin Wang,^{*,[c]}
Alexey A. Popov,^{*,[b, e]} Steven H. Strauss,^{*,[a]} and Olga V. Boltalina^{*,[a]}

Dedicated to Maurizio Prato, on the occasion of his glorious sixtieth birthday and celebration of his contributions to fullerene chemistry

Abstract: Hexasubstituted fullerenes with the skew pentagonal pyramid (SPP) addition pattern are predominantly formed in many types of reactions and represent important and versatile building blocks for supramolecular chemistry, biomedical and optoelectronic applications. Regioselective synthesis and characterization of the new SPP derivative, $C_{60}(CF_3)_4(CN)H$, in this work led to the experimental identification of the new family of “superhalogen fullerene radicals”, species with

the gas-phase electron affinity higher than that of the most electronegative halogens, F and Cl. Low-temperature photoelectron spectroscopy and DFT studies of different $C_{60}X_5$ radicals reveal a profound effect of X groups on their electron affinities (EA), which vary from 2.76 eV ($X=CH_3$) to

4.47 eV ($X=CN$). The measured gas-phase EA of the newly synthesized $C_{60}(CF_3)_4CN$ equals 4.28 (1) eV, which is about 1 eV higher than the EA of Cl atom. An observed remarkable stability of $C_{60}(CF_3)_4CN^-$ in solution under ambient conditions opens new venues for design of air-stable molecular complexes and salts for supramolecular structures of electroactive functional materials.

Keywords: electron affinity • fullerenes • photoelectron spectroscopy • radicals • superhalogen

Introduction

All-carbon closed-cage compounds—fullerenes—represent convenient molecular platforms for design of various materials with the tailored physicochemical properties of funda-

mental and practical importance.^[1] It has been recognized that derivatization has a complex influence on the electron-accepting properties of fullerenes. On one hand, saturation of the fullerene π -system that occurs upon addition of functional groups destabilizes the LUMO and hence decreases electron affinity (EA). On the other hand, electron withdrawing groups tend to increase the EA. Our recent experimental and theoretical studies of the gas-phase EA values and reduction potentials of perfluoroalkylfullerenes (PFAFs) showed that addition patterns (in other words, topology of the π -system) also play an important role^[2c,2d] in determining electronic properties of fullerene derivatives.^[2] For example, the first reduction potentials of different trifluoromethyl fullerene (TMF) $C_{60}(CF_3)_{10}$ isomers span a wide range of 0.50 V (the B3LYP/6-311G*-predicted EA values for these isomers span the range of 0.55 eV), and all studied $C_{60}(CF_3)_{10}$ isomers are better electron acceptors than parent C_{60} .^[2a] Another, even more striking, example worth mentioning concerns two isomers of $C_{60}(CF_3)_6$; one isomer (C_1 symmetry, Schlegel diagram in Figure 1, top) is 0.26 V easier to reduce than C_{60} , whereas the other isomer (C_s symmetry, Schlegel diagram in Figure 1, bottom) is a weaker acceptor than C_{60} (−0.07 V vs. the $C_{60}^{0/-}$ couple) according to cyclic voltammetry.^[2a] This result might be erroneously interpreted as CF_3 groups having opposing electronic effects in these two isomers: it appears that CF_3 groups exhibit electron withdrawing effects in C_1 - $C_{60}(CF_3)_6$ isomer, whereas CF_3 groups have electron donating effects in the C_s isomer.

[a] T. T. Clikeman, Prof. S. H. Strauss, Dr. O. V. Boltalina
Department of Chemistry, Colorado State University
Fort Collins, CO 80523 (USA)
E-mail: steven.strauss@colostate.edu
olga.boltalina@colostate.edu

[b] Dr. A. A. Popov
Department of Electrochemistry and Conducting Polymers
Leibniz Institute for Solid State and Materials Research
01069 Dresden (Germany)
E-mail: a.popov@ifw-dresden.de

[c] Dr. S. H. M. Deng, Dr. X.-B. Wang
Physical Sciences Division, Pacific Northwest National Laboratory
P.O. Box 999, MS K8-88, Richland, Washington 99352 (USA)
E-mail: xuebin.wang@pnnl.gov

[d] Dr. S. Avdoshenko
School of Materials Engineering, Purdue University
Neil Armstrong Hall of Engineering, 701 W. Stadium Avenue
West Lafayette, IN 47907-2045 (USA)

[e] Dr. A. A. Popov
Chemistry Department, Moscow State University
119992 Moscow (Russia)

Supporting information for this article is available on the WWW under <http://dx.doi.org/10.1002/chem.201301234>.

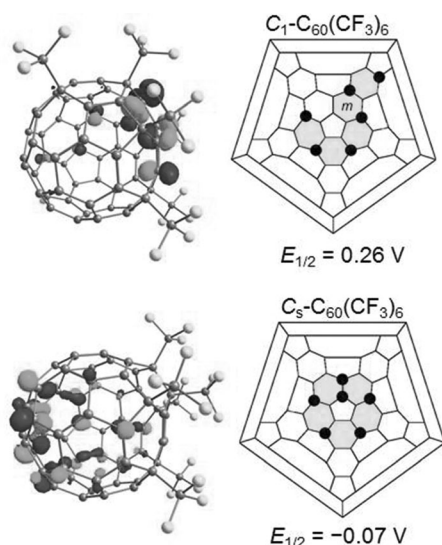


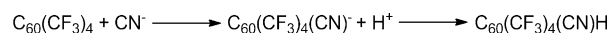
Figure 1. Schlegel diagrams and the DFT-predicted cage carbon atom contributions to the LUMO (dark gray) of C_1 - $C_{60}(\text{CF}_3)_6$ and C_5 - $C_{60}(\text{CF}_3)_6$. The black circles indicate the cage carbon atoms to which the CF_3 groups are attached. The ribbon of edge-sharing m - and p - $C_6(\text{CF}_3)_2$ hexagons are highlighted in light gray.

In fact, the reason for such a different electrochemical behavior lies in the LUMO distributions on these fullerenes: the LUMO in the C_1 isomer is localized in the proximity of the electron withdrawing groups (EWGs), whereas the LUMO in the C_5 isomer is located on the opposite side of the sphere (Figure 1).

What if the addition pattern of a fullerene derivative remains constant, while the nature of the substituents vary (e.g., EWG vs. electron donating group (EDG), or different strength EWGs)? We recently showed that it is possible to determine relative electron-withdrawing effects of R_F substituents in a series of 1,4- $C_{60}(R_F)_2$.^[2b] Here, we will address the electronic effects of functional groups in the most common type of hexasubstituted C_{60} fullerenes, with the skew pentagonal pyramid (SPP) addition pattern (Schlegel diagram is shown on Figure 1, bottom right). We studied several isostructural pentasubstituted derivatives of C_{60} (in radical and anionic forms) C_5 - $C_{60}X_5$, where X is either an EWG, EDG, or both. Such pentasubstituted species were observed as chemical intermediates on the way to the neutral hexasubstituted compounds with the SPP addition pattern. Versatility of the C_5 - $C_{60}X_5$ motif in the organic and organometallic chemistry of fullerenes and importance of related fullerene materials in practical applications necessitate a knowledge and better understanding of the influence of different functional groups on the electron-accepting properties of such derivatives.^[3]

Results and Discussion

First, we performed a two-step, one-flask procedure at room temperature (Scheme 1). The first step involved a selective



Scheme 1. Synthesis of $C_{60}(\text{CF}_3)_4(\text{CN})\text{H}$: addition of CN^- (NEt_4CN) and subsequent addition of H^+ (CF_3COOH) to p^3 - $C_{60}(\text{CF}_3)_4$ in dichloromethane at room temperature.

addition of CN^- group to a tetrasubstituted TMF, $C_{60}(\text{CF}_3)_4$ with a *para-para-para* (p^3) addition pattern (**1**, Figure 2) to obtain $C_{60}(\text{CF}_3)_4(\text{CN})^-$ (**2⁻**) using reaction conditions described earlier.^[4] Compound **1** is a new isomer of the tetrasub-

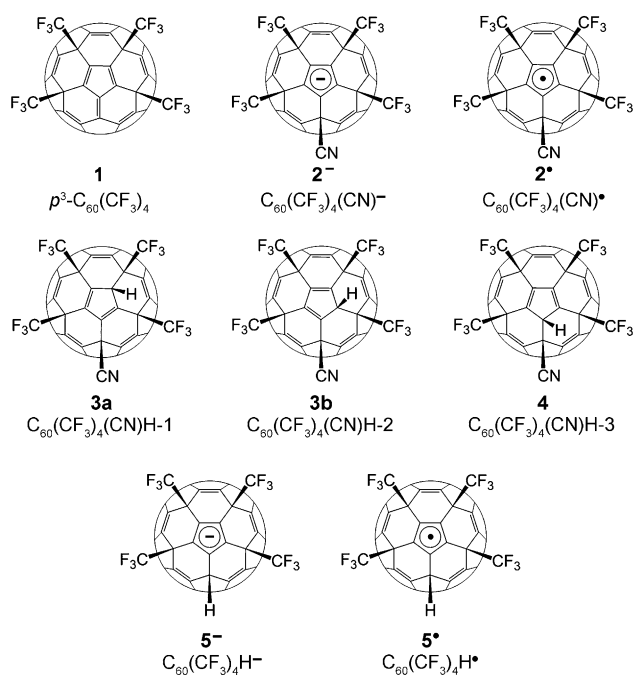


Figure 2. Drawings of molecular structures of fullerene derivatives from this work.

stituted TMF the synthesis and isolation of which was recently made possible due to the use of a specialized gradient-temperature-gas-solid (GTGS) reactor (see the Supporting Information for details).^[5] The choice of this TMF substrate for the regioselective formation of **2⁻** was based on the assumption that high regioselectivity in this process can be achieved due to: 1) the presence of a particularly reactive exocyclic double bond in the fulvene fragment on the cage in the proximity of CF_3 groups in compound **1**; and 2) the stabilizing effect of the aromatic cyclopentadiene anion moiety on the central pentagon. This suggestion was fully confirmed in our synthetic experiments using **1** (Scheme 1).

Addition of a dichloromethane (DCM) solution of NEt_4CN to a brown DCM solution of **1** yielded a brown soluble material, **2⁻**, which exhibited an ^{19}F NMR spectrum with a new set of two CF_3 multiplets (Figure 3B). Subsequent addition of CF_3COOH resulted in the immediate formation of an orange compound (**3**) that was readily purified by HPLC (Figure S1 in the Supporting Information). The product compositions after the first and second steps were

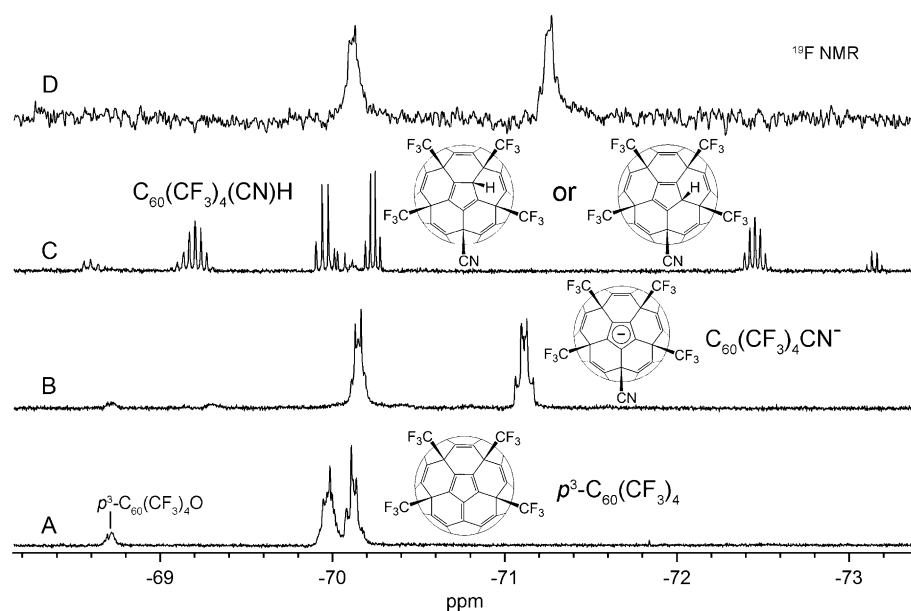


Figure 3. ^{19}F NMR spectra (CD_2Cl_2 ; $\delta(\text{C}_6\text{F}_6) = -164.9$ ppm) showing: the multiplets for: A) $\text{C}_{60}(\text{CF}_3)_4$ (**1**) including a small amount of $\text{C}_{60}(\text{CF}_3)_4\text{O}$ ($\delta = -68.7$ ppm), B) crude $\text{C}_{60}(\text{CF}_3)_4(\text{CN})^-$ (**2** $^-$), C) $\text{C}_{60}(\text{CF}_3)_4(\text{CN})\text{H}$ (**3**), and D) $\text{C}_{60}(\text{CF}_3)_4(\text{CN})^-$ (**2** $^-$) after treatment of **3** with proton sponge.

determined by negative ion atmospheric pressure chemical ionization (NI-APCI) mass spectrometry as $\text{C}_{60}(\text{CF}_3)_4(\text{CN})^-$ (**2** $^-$) and $\text{C}_{60}(\text{CF}_3)_4(\text{CN})\text{H}^-$ (**3** $^-$). Partial dehydrogenation of compound **3** was observed during the mass spectrometry analysis, even under mild APCI MS conditions, as followed from the isotopic distribution analysis of its peak (Figure S2 in the Supporting Information), leading to the generation of **2** $^-$, which is consistent with the higher EA of **2** than that of **3** (see below). Interestingly, the major reaction product **3**, exhibited four well-resolved CF_3 multiplets in the ^{19}F NMR spectrum (Figure 3C). Loss of symmetry in compound **3**, as compared to the symmetric substrate **1** and symmetric anionic species **2** $^-$ formed after addition of CN^- in the first stage, implies that H^+ does not add to the adjacent carbon atom of the central pentagon (**4**, Figure 2) with respect to the carbon atom bonded to the CN group.

The DFT-derived gas-phase energies of three possible isomers with different positions of H atoms in $\text{C}_{60}(\text{CF}_3)_4(\text{CN})\text{H}$ (structures **3a**, **3b**, and **4** on Figure 2) are very close at the PBE/TZ2P level, but the isomer with the H attached near the “internal” CF_3 (structure **3a**) is lower than the asymmetric **3b** and symmetric **4** in energy by 4.5 and 4.9 kJ mol^{-1} , respectively. A similar DFT result was obtained for the hypothetical compound $\text{C}_{60}(\text{CF}_3)_4\text{H}_2$, that is, the isomer with the same addition pattern as **3a**, was 6.4 kJ mol^{-1} lower in energy than an isomer with the same addition pattern as **3b**. In the view of the small energy difference we also performed computations at the B3LYP-D3/def2-TZVP level (with dispersion correction) and found virtually the same values in the gas phase (within 1 kJ mol^{-1}). Solvation energy corrections (computed for DCM using C-PCM model at the B3LYP/6-311G** level) further destabilized the isomer **4** ($\Delta E = 16.9$ kJ mol^{-1}) with respect to the isomer **3a**, however,

the isomer **3a** became 0.8 kJ mol^{-1} more stable than the latter. The barriers of the interconversion between **3a**, **3b**, and **4** all exceed 110–130 kJ mol^{-1} ; such interconversion is not to be expected at room temperature. So far, it is not possible to distinguish **3a** and **3b** based on our experimental data.

We determined the stability of compound **3** and $(\text{NEt}_4)^+$ salt of **2** $^-$ in solution under ambient conditions, and in anaerobic conditions, prior to photoelectron spectroscopy study (see the Supporting Information for more detail). As a solid, compound **3** is stable for weeks under ambient conditions and compound **2** $^-$ is relatively stable in aerobic solution for days. Conversion of **3** back

into **2** $^-$ can be easily realized by removal of proton upon the addition of proton-sponge (1,8-bis(dimethylamino)naphthalene, $\text{C}_{14}\text{H}_{18}\text{N}_2$) in anaerobic conditions, as shown in the ^{19}F NMR spectrum (Figure 3D).

For the experimental determination of gas-phase electron affinity of the compound **3** and TMF substrate **1**, we applied low-temperature photoelectron spectroscopy (PES). Our preliminary APCI mass spectrometry study of the acetonitrile solutions of **1** and **3** indicated that corresponding molecular anionic species can be readily generated. Noteworthy, in the electrospray ion (ESI) source of the mass spectrometer, compound **3** was observed only as fully deprotonated species **2** $^-$ (Figure S2 in the Supporting Information). The EA measurements at 266 nm (4.661 eV) were carried out for acetonitrile solutions of **1** and **3** mixed with appropriate donors using a magnetic-bottle time-of-flight PES coupled with an ESI source and a cryogenic ion-trap for size-selected anions as described elsewhere.^[6] Since sharp peaks are often resolved in the threshold region of photoelectron spectra of fullerene-related anions, the accuracy of EA measurements is around 10 meV, compared to the best cyclic voltammetry experiments (10 mV). Interestingly, the photoelectron spectrum of the anion produced from **1** consists of two features, one at $3.21(\pm 0.01)$ eV, and the second one, more pronounced, at $3.96(\pm 0.01)$ eV, which indicates that two anionic species with considerably different electron binding energies contribute to the photoelectron detachment process (Figure 4). It is reasonable to suggest that the peak observed at 3.21 eV is due to the parent molecular $\text{C}_{60}^-(\text{CF}_3)_4$ anion, whereas the peak at 3.96 eV is likely to be due to a hydrogenated anion, $\text{C}_{60}(\text{CF}_3)_4\text{H}^-$ (structure **5** $^-$, Figure 2) based on the observed ion signal width. The most likely explanation for the formation of such pentasubstituted

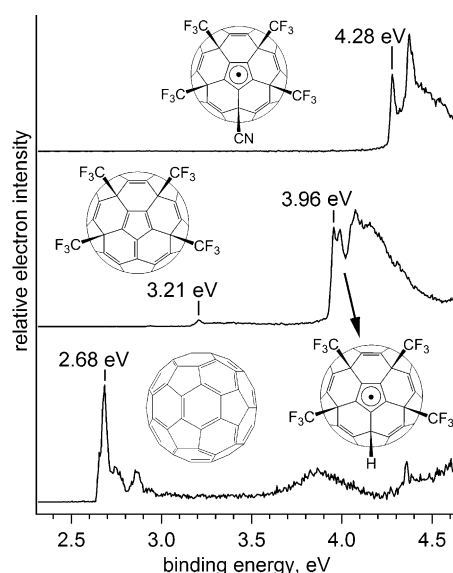


Figure 4. The low temperature (12 K) photoelectron spectrum at 266 nm of $C_{60}(CF_3)_4(CN)^-$ (**2**⁻, top), $C_{60}(CF_3)_4^-$ and $C_{60}(CF_3)_4H^-$ (**1**⁻ and **5**⁻, middle); and C_{60}^- (at 68 K; bottom, first reported in ref. [8])

anion is a very high reactivity of the anionic form of **1** in solution that leads to hydrogen abstraction from the solvent (not thoroughly dry) or from the ESI process, which occurred at the ambient environment with a certain amount of water vapor and formation of the particularly stable anion (**1**⁻+H), **5**⁻, bearing an aromatic cyclopentadiene moiety. Within the current instrumental mass resolution, it is difficult to separate anionic beams with m/z 996 (**1**⁻) and 997 (**5**⁻), but we were able to see change of spectral area ratio of the low and high binding energy features corresponding to these two species ranging from 0.039 to 0.089 in five different PES studies by selecting different portions of the ion clouds containing both m/z 996 (**1**⁻; minor) and 997 (**5**⁻; majority). Please note these ratios cannot be directly translated into the ion population of **1**⁻ over **5**⁻ because the detachment cross sections of these two anionic species may not be the same. We can also safely rule out that formation of **5**⁻ could occur after mass selection because of the absence of hydrogen atom source: only N_2 molecules constitute the background gas (at vacuum as high as 10^{-8} torr). Our interpretation of the PES spectrum of **1** is strongly supported by the theoretical calculations. The DFT-derived EA of **1** is 3.10 eV, whereas the EA value of **5** was calculated as 3.73 eV. Such a considerable difference between the EA values of the two species is explained by two factors: 1) EA of the open shell molecular species is known to be higher than that of closed-shell species;^[7] 2) addition of H atom to $C_{60}(CF_3)_4^-$ leads to a significant stabilization of the structure due to the formation of aromatic moiety as shown for structure **5**⁻ (Figure 2).

The PES spectrum of **3** consists of only one strong peak at 4.28 eV. Slightly different mass selection for the ion beam generated from a solution of **3** has been also carried out, which indicated that only one ion species existed, C_{60}^-

(CF_3)₄(CN)⁻ (**2**⁻), a product of complete deprotonation of **3** under applied experimental conditions, in agreement with the preliminary ESI MS results for **3** discussed above. Therefore, the EA of $C_{60}(CF_3)_4(CN)^-$ (**2**) was measured from the first resolved peak to be 4.28(±0.01) eV.

Table 1 contains adiabatic EA value for **1** (measured in this work) and, for comparison, earlier reported EA values

Table 1. Experimental and DFT-calculated EA values [eV], $E_{1/2}$ (V, vs. C_{60}^{0-}) and $E(LUMO)$ (eV, vs. C_{60}) values of some closed-shell TMFs.

	EA (exp)	EA (DFT) ^[a,b]	$E_{1/2}$ (exp) ^[c]	$E_{1/2}$ (DFT) ^[c,d]	E (LUMO) ^[c,e]
C_{60}	2.68(1) ^[f]	2.64 ^[a]	0	0	0
$C_{60}(CF_3)_2$	2.92(1) ^[g]	2.77 ^[a]	0.11	0.09	-0.213
$p^3-C_{60}(CF_3)_4$	3.21(1)	3.10 ^[a]	(irrev.)	0.29	-0.460
$pmp-C_{60}(CF_3)_4$	–	2.96 ^[b,c]	0.17	0.17	-0.303
$S_6-C_{60}(CF_3)_{12}$	2.57(17) ^[h]	2.65 ^[b,h]	-0.16	-0.21	0.101

[a] B3LYP/def2-TZVP//PBE/TZ2P level; [b] B3LYP/6-311G*//PBE/TZ2P level; [c] See ref. 2a; [d] estimated based on the linear correlation found between PBE-derived LUMO energies and experimentally measured redox potentials; [e] PPE/TZ2P level; $E_{1/2}$ and $E(LUMO)$ are relative to C_{60} values; [f] See ref. 8; [g] See ref. 2b; [h] See ref. 9.

of some closed-shell TMFs and C_{60} , and the DFT-calculated EA, $E_{1/2}$, and $E(LUMO)$ values. Importantly, relative trends in electron acceptor strength for the listed compounds based either on their EA values, $E_{1/2}$ or $E(LUMO)$ are in qualitative agreement, that is, acceptor strength increases in the order: $p^3-C_{60}(CF_3)_4 > pmp-C_{60}(CF_3)_4 > C_{60}(CF_3)_2 > C_{60} > S_6-C_{60}(CF_3)_{12}$.

The EA of the isomerically pure TMF, $p^3-C_{60}(CF_3)_4$ (**1**), is the first value for a TMF with more than two CF_3 groups measured with the high precision of 0.01 eV, compare with the error of 0.17 eV reported for $S_6-C_{60}(CF_3)_{12}$.^[9] We also note that the EA data for $C_{60}(CF_3)_{10}$ were obtained using a sample comprised of a mixture of isomers with unknown composition and with high uncertainty of about 0.2 eV^[9,10] and hence they were not used in this analysis. The EA value of 3.21 eV measured for $p^3-C_{60}(CF_3)_4$ in this work is 0.53 eV higher than measured for C_{60} ,^[10] this confirms the predicted high electron affinity for the p^3 addition pattern in C_{60} made in our earlier studies and serves as good validation of the DFT method used.^[2a] Experimental EA values for $C_{60}(CF_3)_4H$ (**5**) and $C_{60}(CF_3)_4CN$ (**2**) are also reliably reproduced by the results of DFT calculations (Table 2). Although the absolute EA values are systematically underestimated by about 0.2 eV, the difference between **5** and **2** is predicted with very high precision ($\Delta E_{DFT}=0.34$ eV vs. $\Delta E_{exp}=0.32$ eV).

Currently, there are only a few examples when the effect of different functional groups could be determined experimentally from the measurements of reduction potentials or EA values of fullerene derivatives with the same addition pattern.^[2b,11] For example, Wudl and co-workers have shown that $C_{60}(CN)_2$ is easier to reduce than isostructural $C_{60}H(CN)$ by 0.07–0.12 V.^[11,12] For $C_{60}(CN)_4$ and $C_{60}H(CN)_3$, the same authors reported the difference of 0.15 V, however,

Table 2. Experimental and DFT electron affinities values [eV] of $C_{60}X_5$ radicals and NICS values in $C_{60}X_5^-$ anions.^[a]

$C_{60}X_5$	EA (exptl)	EA (DFT)	NICS (Cp)	NICS (center)	NICS (cage)
$C_{60}(CH_3)_5$		2.76	−5.8	−11.9	12.2
$C_{60}H_5$		2.79	−12.8	−12.0	10.4
$C_{60}(Ph)_5$		3.07	−5.2	−12.3	11.5
$C_{60}(CF_3)_4H$	3.96(1)	3.73	−10.2	−12.9	11.0
$C_{60}(CF_3)_5$		3.99	−10.0	−13.1	10.7
$C_{60}(C_2F_5)_5$		4.02	−9.0	−13.2	10.9
$C_{60}(CF_3)_4CN$	4.28(1)	4.07	−10.2	−13.3	10.8
$C_{60}(CN)_5$		4.47	−11.7	−13.6	10.7

[a] EA computed at B3LYP/def2-TZVP level, NICS at the PBE/A2 level, coordinates are optimized at the PBE/TZ2P level.

the measurements were performed for a mixture of isomers.^[12] Results of our study show that the difference of EA values of $C_{60}(CF_3)_4CN$ and $C_{60}(CF_3)_4H$ radicals can be as high as 0.32 eV! The electrochemical data on the effect of the substituents in the fullerene derivatives with the SPP structures are even more scarce,^[3a] despite abundance of such structures among the synthesized organic derivatives.

After validation of the DFT calculations of EA values discussed above, we performed an extended analysis of EA values of the $C_{60}X_5$ compounds with different addends based on the DFT-computed data (Table 2). Computations show that depending on the addend, EA of $C_{60}X_5$ radical can vary within the range of 1.71 eV, from 2.76 eV for $X=CH_3$ to exceptionally high value of 4.47 eV for $X=CN$. When $X=H$, EA increases by only 0.03 eV versus $C_{60}(CH_3)_5$, whereas EA of $C_{60}(Ph)_5$ is increased to 3.07 eV. Note that the DFT-computed EA of C_{60} is 2.64 eV, and hence the difference of computed EA values of C_{60} and $C_{60}(Ph)_5$, 0.43 eV, is very close to the experimentally measured difference of their reduction potentials in THF.^[3a] $C_{60}(CF_3)_5$ and $C_{60}(C_2F_5)_5$ exhibit almost identical values of 3.99 and 4.02 eV, respectively. Interestingly, the difference between these two values, 0.03 eV, is the same as the difference between the experimentally determined EA values of $C_{60}(CF_3)_2$ and $C_{60}(C_2F_5)_2$ ^[2b] and thus it confirms that the electron withdrawing effect of R_F groups increases slightly in going to higher R_F homologues. Importantly, one fifth of the difference between EA values of $C_{60}H_5$ and $C_{60}(CN)_5$, 0.34 eV, is equal to the H-to-CN increment found for the EA values of the $C_{60}(CF_3)_4X$ ($X=H, CN$) pair.

One of the factors resulting in the high electron affinity of $C_{60}X_5$ radicals is the formation of the aromatic cyclopentadiene anion. In the earlier theoretical considerations, it was hypothesized that high EA of highly fluorinated fullerene, $C_{60}F_{34}$, could be due to the presence of two cyclopentadiene moieties in its structure.^[xxx] In this work, in order to analyze if there is a correlation between the addend X and aromaticity, we have computed nucleus-independent chemical shifts (NICS) at several points of $C_{60}X_5^-$ anions, namely at the center of the cyclopentadiene ring, at the center of the opposite cage ring, and the center of C_{60} cage. These calculations showed that, as anticipated, the cyclopentadiene ring is aromatic with NICS values of −5 to −13 ppm, whereas the

opposite pentagon is always antiaromatic (positive NICS values of 10–12 ppm). Interestingly, NICS values in the center of the cage are even more negative than in the center of the cyclopentadiene ring. Moreover, they exhibit a perfectly linear correlation with the EA values showing that the “bulk” aromaticity of the cage is related to the addend in the same way as EA (the higher EA, the more negative NICS). At the same time, the values in the center of the pentadienyl ring are less correlated with EA (presumably due to the local shielding effects of the addends).

Conclusion

We have prepared and characterized $C_{60}(CF_3)_4(CN)H$, a rare representative of a fullerene derivative with the SPP addition pattern in which five substituents are strong electron withdrawing groups. This type of SPP derivative possesses good air stability, in contrast to the counterparts with electron donating groups, and exceptionally high electron affinity of the respective radicals, and hence, high thermodynamic stability of the anions. Due to these unique properties, such SPP derivatives of TMFs may become increasingly important building blocks in the molecular and supramolecular designs of the electroactive functional materials.

Experimental Section

General information: All reagents and solvents were reagent grade or better. Net_4CN and CF_3COOH were obtained from Sigma-Aldrich and were used as received. Proton-sponge was obtained from Sigma-Aldrich and purified by sublimation prior to use. All solvents were dried by standard techniques and stored under purified dinitrogen. The synthesis of compound **1** is described in the Supporting Information. All manipulations of $C_{60}(CF_3)_4^-$ were carried out under an atmosphere of purified dinitrogen by using glovebox techniques. HPLC analyses and purifications were carried out by using Shimadzu HPLC instrumentation (CBM-20A control module, SPD-20A UV detector set to 300 nm, LC-6AD pump, manual injector valve) equipped with a semi-preparative 10 mm I.D. × 250 mm Cosmosil Buckyrep or Cosmosil Buckyrep-M column (Nacalai Tesque, Inc.). ^{19}F NMR spectra were recorded by using a Varian 400 spectrometer operating at 376.5 MHz (C_6F_6 internal standard, $\delta = -164.9$ ppm). Negative-ion APCI and ESI mass spectra were recorded by using a Finnigan 2000 LCQ-DUO spectrometer. The samples were injected as approximately 1:1 DCM/MeCN solutions; the mobile phase was MeCN.

Generation of $Net_4[C_5-C_{60}(CF_3)_4(CN)]$ in solution and the isolation of $C_1-C_{60}(CF_3)_4(CN)H$: Under an atmosphere of purified N_2 , the $C_5-C_{60}(CF_3)_4(CN)^-$ anion was generated by adding an aliquot of a colorless 25.8 mm DCM solution of Net_4CN (1.10 mL, 7.1 μ mol CN^-) to a brown solution of **1** (7.1 mg, 7.1 μ mol) in dry DCM (8.3 mL) at 23(2) °C and the color remained brown. After 20 min an excess of trifluoroacetic acid (~1000 equiv) was added dropwise and the solution immediately turned orange. The reaction mixture was then exposed to air, passed through silica gel in DCM, and the solvent was removed. The brown solid was then purified by HPLC (semi-preparative 10 mm I.D. × 250 mm Cosmosil Buckyrep column (Nacalai Tesque, Inc.), toluene/heptane = 4:1, 5 mL min^{−1}, $t_R = 10.9$ min). ^{19}F NMR (CD_2Cl_2): $\delta = -69.2$ (apparent septet (as), int. 3), -69.9 (q, int. 3, $J_{FF} = 11(1)$ Hz), -72.2 (q, int. 3, $J_{FF} = 11(1)$ Hz), -72.5 ppm (as, int. 3). Note that colorless DCM solutions of

NEt₄CN become yellow after one day, so fresh solutions were prepared for the reaction.

DFT calculations: Optimization of atomic coordinates of all studied species and GIAO computations of NICS values were performed at the PBE/TZ2P level using Priroda code.^[q1] Addition point-energy computations at the B3LYP-D3/def2-TZVP level were performed using ORCA suite.^[q2] Solvation energy corrections were computed using Firefly (version 8.0) at the B3LYP/6-311G** level.^[14–16]

Acknowledgements

We thank US NSF (CHE-1012468), NIH (5R21A140080-03) and the Colorado State University Research Foundation for generous support. The PES work was supported by the US Department of Energy (DOE), Division of Chemical Sciences, Geosciences and Biosciences, Office of Basic Energy Sciences and was performed at the EMSL, a national scientific user facility sponsored by DOE's Office of Biological and Environmental Research and located at Pacific Northwest National Laboratory, which is operated for DOE by Battelle. A.A.P. acknowledges DFG (project PO1602/1-1) for financial support and Ulrike Nitzsche for assistance with local computational resources in IFW Dresden. Research Computing Center of Moscow State University and Jülich Supercomputing Center are acknowledged for computing time on supercomputers "SKIF-Chebyshev" and JUROPA, respectively. S.M.A. acknowledges Rosen Center for Advanced Computing (RCAC) at Purdue for computational facilities.

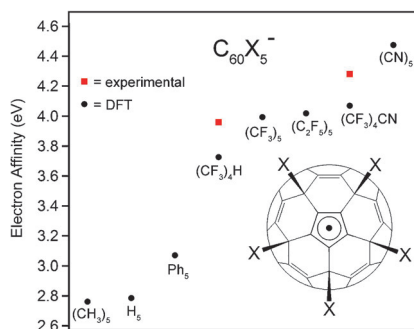
- [1] a) A. Hirsch, M. Brettreich, *Fullerenes: Chemistry and Reactions*, Wiley-VCH, Weinheim, **2005**; b) B. C. Thompson, J. M. J. Frechet, *Angew. Chem.* **2008**, *120*, 62–82; *Angew. Chem. Int. Ed.* **2008**, *47*, 58–77.
- [2] a) A. A. Popov, I. E. Kareev, N. B. Shustova, E. B. Stukalin, S. F. Lebedkin, K. Seppelt, S. H. Strauss, O. V. Boltalina, L. Dunsch, *J. Am. Chem. Soc.* **2007**, *129*, 11551–11568; b) I. V. Kuvychko, J. B. Whitaker, B. W. Larson, T. C. Folsom, N. B. Shustova, S. M. Avdoshenko, Y. S. Chen, H. Wen, X. B. Wang, L. Dunsch, A. A. Popov, O. V. Boltalina, S. H. Strauss, *Chem. Sci.* **2012**, *3*, 1399–1407; c) N. Martin, L. Sánchez, B. Illescas, I. Pérez, *Chem. Rev.* **1998**, *98*, 2527–2548; d) I. V. Kuvychko, J. B. Whitaker, B. W. Larson, T. C. Folsom, N. B. Shustova, S. M. Avdoshenko, Y. S. Chen, H. Wen, X. B. Wang, L. Dunsch, A. A. Popov, O. V. Boltalina, S. H. Strauss, *Chem. Sci.* **2012**, *3*, 1399–1407; B. M. Illescas, N. Martin, *Comptes Rendu de Chimie*, **2006**, *9*, 1038–1050.
- [3] a) H. Iikura, S. Mori, M. Sawamura, E. Nakamura, *J. Org. Chem.* **1997**, *62*, 7912–7913; b) M. Sawamura, Y. Kuninobu, M. Toganoh, Y. Matsuo, M. Yamanaka, E. Nakamura, *J. Am. Chem. Soc.* **2002**, *124*, 9354–9355; c) M. Sawamura, N. Nagahama, M. Toganoh, U. E. Hackler, H. Isobe, E. Nakamura, S. Q. Zhou, B. Chu, *Chem. Lett.* **2000**, 1098–1099; d) Y. Kuninobu, Y. Matsuo, M. Toganoh, M. Sawamura, E. Nakamura, *Organometallics* **2004**, *23*, 3259–3266; e) Y. Matsuo, Y. Kuninobu, S. Ito, E. Nakamura, *Chem. Lett.* **2004**, *33*, 68–69; f) I. E. Kareev, N. B. Shustova, I. V. Kuvychko, S. F. Lebedkin, S. M. Miller, O. P. Anderson, A. A. Popov, S. H. Strauss, O. V. Boltalina, *J. Am. Chem. Soc.* **2006**, *128*, 12268–12280; g) I. V. Kuvychko, N. B. Shustova, S. M. Avdoshenko, A. A. Popov, S. H. Strauss, O. V. Boltalina, *Chem. Eur. J.* **2011**, *17*, 8799–8802; h) P. A. Troshin, E. A. Khakina, A. S. Peregudov, D. V. Konarev, I. V. Soulimenkov, S. M. Peregudova, R. N. Lyubovskaya, *Eur. J. Org. Chem.* **2010**, 3265–3268; i) A. G. Avent, P. R. Birkett, J. D. Crane, A. D. Darwish, G. J. Langley, H. W. Kroto, R. Taylor, D. R. M. Walton, *J. Chem. Soc. Chem. Commun.* **1994**, 1463–1464; j) P. R. Birkett, A. G. Avent, A. D. Darwish, H. W. Kroto, R. Taylor, D. R. M. Walton, *J. Chem. Soc. Chem. Commun.* **1993**, 1230–1232.
- [4] T. T. Clikeman, I. V. Kuvychko, N. B. Shustova, Y.-S. Chen, A. A. B. Popov, O. V. Boltalina, S. H. Strauss, *Chem. Eur. J.* **2013**, *19*, 5070–5080.
- [5] I. V. Kuvychko, J. B. Whitaker, B. W. Larson, R. S. Raguindin, K. J. Suhr, S. H. Strauss, O. V. Boltalina, *J. Fluorine Chem.* **2011**, *132*, 679–685.
- [6] X. B. Wang, L. S. Wang, *Rev. Sci. Instrum.* **2008**, *79*, 073108/073101.
- [7] X.-B. Wang, C. Chi, M. Zhou, I. V. Kuvychko, K. Seppelt, A. A. Popov, S. H. Strauss, O. V. Boltalina, L.-S. Wang, *J. Phys. Chem. A* **2010**, *114*, 1756–1765.
- [8] X. B. Wang, H. K. Woo, L. S. Wang, *J. Chem. Phys.* **2005**, *123*, 051106-1-4.
- [9] N. I. Gruzinskaya, V. E. Aleshina, A. Y. Borshchevskii, L. N. Sidorov, *J. Anal. Chem.* **2010**, *65*, 1328–1332.
- [10] a) V. Y. Markov, V. E. Aleshina, A. Y. Borshchevskii, R. V. Khatymov, R. F. Tuktarov, A. V. Pogulay, A. L. Maximov, S. V. Kardashev, I. N. Ioffe, S. M. Avdoshenko, E. I. Dorozhkin, A. A. Goryunkov, D. V. Ignat'eva, N. I. Gruzinskaya, L. N. Sidorov, *Int. J. Mass Spectrom.* **2006**, *251*, 16–22; b) A. Y. Borshchevskii, V. E. Aleshina, V. Y. Markov, E. I. Dorozhkin, L. N. Sidorov, *Inorg. Mater.* **2005**, *41*, 1318–1326.
- [11] M. Keshavarz-K, B. Knight, G. Srdanov, F. Wudl, *J. Am. Chem. Soc.* **1995**, *117*, 11371–11372.
- [12] B. Jousselme, G. Sonmez, F. Wudl, *J. Mater. Chem.* **2006**, *16*, 3478–3482.
- [13] I. N. Ioffe, S. M. Avdoshenko, O. V. Boltalina, L. N. Sidorov, K. Berndt, J. M. Weber, *Int. J. Mass Spectrom.* **2005**, *243*, 223.
- [14] a) D. N. Laikov, Y. A. Ustynuk, *Russ. Chem. Bull.* **2005**, *54*, 820–826; b) D. N. Laikov, *Chem. Phys. Lett.* **1997**, *281*, 151–156.
- [15] F. Neese, *WIREs Comput. Mol. Sci.* **2012**, *2*, 73–78.
- [16] A. A. Granovsky, Firefly, version 8.0.0, **2013**, <http://classic.chem.msu.su/gran/firefly/index.html>.

Received: April 2, 2013

Revised: July 3, 2013

Published online: ■■■■, 0000

Electric balls: Synthesis, low-temperature photoelectron spectroscopy, and DFT studies of different $C_{60}X_5$ radicals reveal a profound effect of X groups on their electron affinities (EA), which span the range of nearly 2 eV as shown on graph. When $X = R_F$ or CN, electron affinity of $C_{60}X_5$ exceeds that of the most electronegative atoms, F and Cl.



Fullerene Superhalogens

*T. T. Clikeman, S. H. M. Deng,
S. Avdoshenko, X.-B. Wang,*
A. A. Popov,* S. H. Strauss,*
O. V. Boltalina**



**Fullerene “Superhalogen” Radicals:
the Substituent Effect on Electronic
Properties of 1,7,11,24,27- $C_{60}X_5$**

